Proc. Natl. Acad. Sci. USA
Vol. 93, pp. 7496–7501, July 1996
Biochemistry

Crystal structure of D-amino acid oxidase: A case of active site mirror-image convergent evolution with flavocytochrome b_2

(density averaging/flavoenzyme/redox catalysis/stereospecificity)

ANDREA MATTEVI*†, MARIA ANTONIETTA VANONI‡, FLAVIA TODONE*, MENICO RIZZI*, ALEX TEPLYAKOV§, ALESSANDRO CODA*¶, MARTINO BOLOGNESI*‖, AND BRUNO CURTI‡¶

*Dipartimento di Genetica e Microbiologia, Università di Pavia, Via Abbiategrasso 207, 27100 Pavia, Italy; ‡Dipartimento di Fisiologia e Biochimica Generali, Università di Milano, Via Celoria 26, 20133 Milan, Italy; §European Molecular Biology Laboratory Outstation, Deutsches Elektronen Synchrotron, 22063 Hamburg, Germany; ‖Dipartimento di Fisica and IST Centro per le Biotecnologie Avanzate, Università di Genova, Viale Benedetto XV 10, 16132 Genoa, Italy; and ¶Centro Interuniversitario per lo Studio delle Macromolecole Informazionali

Communicated by Vincent Massey, University of Michigan Medical School, Ann Arbor, MI, January 19, 1996 (received for review December 9, 1995)

ABSTRACT **D-amino acid oxidase is the prototype of the FAD-dependent oxidases. It catalyses the oxidation of D-amino acids to the corresponding α-ketoacids. The reducing equivalents are transferred to molecular oxygen with production of hydrogen peroxide. We have solved the crystal structure of the complex of D-amino acid oxidase with benzoate, a competitive inhibitor of the substrate, by single isomorphous replacement and eightfold averaging. Each monomer is formed by two domains with an overall topology similar to that of *p*-hydroxybenzoate hydroxylase. The benzoate molecule lays parallel to the flavin ring and is held in position by a salt bridge with Arg-283. Analysis of the active site shows that no side chains are properly positioned to act as the postulated base required for the catalytic carboanion mechanism. On the contrary, the benzoate binding mode suggests a direct transfer of the substrate α-hydrogen to the flavin during the enzyme reductive half-reaction. The active site of D-amino acid oxidase exhibits a striking similarity with that of flavocytochrome b_2, a structurally unrelated FMN-dependent flavoenzyme. The active site groups of these two enzymes are in fact superimposable once the mirror-image of the flavocytochrome b_2 active site is generated with respect to the flavin plane. Therefore, the catalytic sites of D-amino acid oxidase and flavocytochrome b_2 appear to have converged to a highly similar but enantiomeric architecture in order to catalyze similar reactions (oxidation of α-amino acids or α-hydroxy acids), although with opposite stereochemistry.**

Since the description of D-amino acid oxidase (EC 1.4.3.3; DAAO) activity in mammalian tissues by Krebs in 1935 (1), DAAO has been the subject of a number of biochemical, spectroscopic, and kinetic investigations, becoming the prototype for the oxidase class of the flavin-containing enzymes [for a recent review, see ref. 2]. Its primary structure has been determined and its gene has been cloned (3, 4). Its kinetic and mechanistic properties have been studied in detail by a variety of techniques, while information on the topology of the active site and on its three-dimensional structure have only been derived from chemical modification studies and site-directed mutagenesis of selected residues. Based on these approaches, a catalytic mechanism for DAAO has been proposed, although definitive evidence against alternative mechanisms has not been found (refs. 2 and 5 and references therein).

The enzyme catalyzes the oxidation of D-α-amino acids into the corresponding α-ketoacids. The reaction formally proceeds according to the following scheme:

$$RCHNH_2COOH + E\text{-}FAD \rightarrow RC{=}NHCOOH + E\text{-}FADH_2 \quad [1]$$

$$E\text{-}FADH_2 + O_2 \rightarrow E\text{-}FAD + H_2O_2 \quad [2]$$

$$RC{=}NHCOOH + H_2O \rightarrow RCOCOOH + NH_3 \quad [3]$$

The reductive half reaction (Eq. **1**), in which the noncovalently bound FAD becomes reduced, is followed by the oxidative step in which FAD is reoxidized by molecular oxygen, with the release of hydrogen peroxide (Eq. **2**). The imino acid product spontaneously hydrolyzes to the ketoacid in a nonenzymatic process (Eq. **3**). DAAO displays a broad substrate specificity, with a preference for D-amino acids bearing hydrophobic side chains up to four carbon-atoms long, followed by those carrying polar and aromatic groups (6). The enzyme exhibits very low activity toward basic amino acids and it does not oxidize those with an acidic side chain. These are oxidatively deaminated by a specific enzyme, D-aspartate oxidase, which shares 50% sequence identity with DAAO (7). Both oxidases are highly stereospecific, and unable to metabolize L-amino acids.

The biological role of DAAO, a peroxisomal enzyme, is controversial (2). The recent detection of significant quantities of D-amino acids in various mammalian tissues suggests that DAAO is a detoxifying agent that removes the D-amino acids deriving from either exogenous or endogenous sources (8). Peptides incorporating D-amino acids have been found not only in prokaryotes, where they are common, but also in several vertebrates, in a few cases as neuropeptides produced by nerve cells (9). In this context, the presence of high levels of DAAO activity in human cerebellum is in keeping with the detection of D-amino acids in the human brain (10).

We have now succeeded in solving the crystal structure of pig kidney DAAO in complex with the competitive inhibitor benzoate. The enzyme is a dimer comprising 2 × 347 amino acids and a molecule of noncovalently bound FAD per subunit. The inhibitor has well-defined electron density which allows the identification and description of the active site.

MATERIALS AND METHODS

The methodology employed in the crystallization and structure determination will be described in detail elsewhere. Briefly, DAAO isolated from pig kidneys (11) was crystallized by the hanging-drop method under conditions similar to those reported by Bolognesi *et al.* (12). Protein solutions (50 mg protein/ml) containing 2 mM sodium benzoate were equilibrated by vapor diffusion against a reservoir containing 0.5 M ammonium succinate, 100 mM Tris·HCl (pH 8.3) at 28°C. The crystals belong to orthorhombic space group $C222_1$ with cell dimensions a = 328 Å, b = 138 Å, c = 201 Å, and four dimers (296,000 Da) in the asymmetric unit. All data sets used for structure determination were collected at room temperature on a Raxis-II imaging plate

The publication costs of this article were defrayed in part by page charge payment. This article must therefore be hereby marked "*advertisement*" in accordance with 18 U.S.C. §1734 solely to indicate this fact.

Abbreviations: DAAO, D-amino acid oxidase; PHBH, p-hydroxybenzoate hydroxylase; FCB, flavocytochrome b_2; SIR, single isomorphus replacement.

Data deposition: The atomic coordinates have been deposited in the Protein Data Bank, Chemistry Department, Brookhaven National Laboratory, Upton, NY 11973 (reference 1KIF).

†To whom reprint requests should be addressed. e-mail: mattevi@ipvgen.unipv.it.

system using CuKα radiation (Table 1). The 2.6 Å native data set employed in the refinement was collected at the X31 beam line of the European Molecular Biology Laboratory/Deutsches Elektronen Synchrotron (Hamburg). This data set was incomplete at low resolution and therefore was merged with a data set collected on the in-house Raxis-II system (Table 1). The images were evaluated using MOSFLM (A. Leslie, personal communication), while the CCP4 suite (13) was used in data reduction. Only one heavy atom derivative was sufficient for structure determination and it was obtained by soaking crystals in a saturated solution of *p*-chloromercury benzoate. The isomorphous difference Patterson map was interpreted using SHELX-90 (14) and the heavy atom parameters were refined using the program MLPHARE (13). The structure solution was based on the resulting single isomorphous replacement (SIR) map that allowed identification of the protein boundaries. A fragment of the electron density map was used as a search probe in a molecular replacement calculation that led to the identification of the noncrystallographic symmetry operators. These calculations were carried out using programs ALMN (13) and GLRF (15). The SIR phases were refined and gradually extended to 3.0 Å by eightfold averaging and solvent flattening using the program package DEMON (16). The resulting map was of excellent quality (Fig. 1), allowing us to trace the polypeptide chain. An initial model was built using program O (17) and was subjected to TNT (18) least-squares refinement to give a crystallographic *R*-factor of 22.8% for all 119,237 measured reflections up to 2.6 Å (no σ cut-off was applied; Table 2). The free *R*-factor (20) for 1000 reflections omitted from the refinement is 24.5%. In the least-squares refinement, the eight subunits present in the asymmetric unit were constrained to be identical, leading to a number of observations per number of parameters ratio of about 12. A total of 270 ordered water molecules were added at positions with density $>1\sigma$ in the 2Fo-Fc map and $>3\sigma$ in the Fo-Fc map. All these water molecules are engaged in at least two hydrogen bonds with a protein or a solvent atom. The final model has good stereochemistry (Table 2), and all residues are within energetically favored regions of the Ramachandran plot (19).

RESULTS AND DISCUSSION

Overall Structure. The DAAO subunit is schematically shown in Fig. 2*a*. Each subunit is clearly divided into two domains, the FAD binding domain (residues 1–63, 141–183, 294–339) with the dinucleotide binding fold observed in several flavoenzymes (22), and the interface domain (residues 64–140, 184–293) characterized by a large eight-stranded mixed β-sheet (Fig. 2*b*). The C-terminal residues 340–347 are disordered and not visible in the electron density map. They belong to a 2-kDa C-terminal peptide that is cleaved off by limited proteolysis without affecting the catalytic properties of

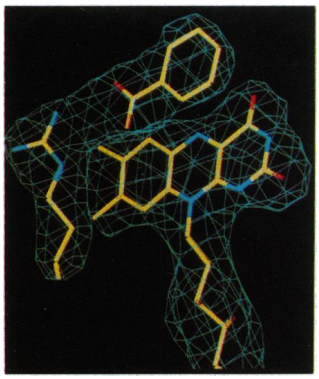

FIG. 1. Electron density for FAD, benzoate, and Arg-283 calculated at 3.0 Å after phase extension by eightfold averaging. The contour level is 1σ. The refined final model is colored by atom type: C, yellow; N, blue; O; red. Produced with program O (17).

the enzyme (23). DAAO forms a dimer of tightly interacting subunits related by an exact twofold axis (Fig. 2*c*). Approximately 15% (1512 Å^2) of the monomer accessible surface is buried upon dimerization with the contact area between the subunits entirely formed by the interface domain.

The overall topology of DAAO resembles that of *p*-hydroxybenzoate hydroxylase (PHBH) (24), cholesterol oxidase (25), and glucose oxidase (26). Superpositions using the program DALI (27) indicate that the similarity is higher for PHBH (rms of 3.5 Å for 249 α-carbons, 15% sequence identity for the residues used in the superposition) than for glucose oxidase (4.6 Å for 248 Cα pairs with 10% sequence identity) and cholesterol oxidase (4.4 Å for 223 Cα pairs with 13% sequence identity). This observation implies that this class of related flavoenzymes can be grouped into two subfamilies: DAAO and PHBH form the first, glucose oxidase and cholesterol oxidase form the second. With respect to PHBH, the topology of DAAO mainly differs for an additional strand (βI2, see Fig. 2*b*) on the β-sheet of the interface domain and for the replacement of the so-called β-meander (22) on the FAD binding domain by helix αF3. Moreover, DAAO lacks the small C-terminal domain present in PHBH.

sz;9q;.5qFAD Binding. The binding of FAD in DAAO is similar to that observed in PHBH. The prosthetic group adopts an extended conformation with the flavin ring located at the interface between the domains of the subunit. The FAD in the DAAO–benzoate complex is completely embedded within one monomer, and there are no cofactor atoms accessible to the solvent (Fig. 2*a*). Nearly all hydrogen-bond donors and acceptors of FAD interact with a protein or a well-ordered solvent atom (Fig. 3). In common with other dinucleotide-

Table 1. Data collection and SIR statistics

Data set	No. of reflections: Total	No. of reflections: Unique (% complete)	R_{merge},* %	MFID,* %	Sites	$\|F_H\|/E$*	R_c*
Native†							
Overall	592,028	119,237 (86)	9.5				
25.0–2.8 Å	564,910	106,921 (93)	9.0				
2.8–2.6 Å	27,118	123,16 (45)	27.0				
PCMB†							
25.0–4.2 Å	196,806	32,514 (97)	7.8	17.1	12	1.56	0.66

*$R_{merge} = \Sigma|I_j - <I_j>|/\Sigma<I_j>$, where I_j is the intensity of an observation of reflection *j* and $<I_j>$ is the average intensity for reflection *j*. MFID = mean fractional isomorphous difference, $\Sigma||F_{PH}|-|F_P||/\Sigma|F_P|$, where $|F_P|$ and $|F_{PH}|$ are the structure factor amplitudes of the native and the derivative, respectively. $R_c = \Sigma||F_{PH} \pm F_P| - F_H|/\Sigma|F_{PH} \pm F_P|$. $|F_H|/E$ = phasing power, *E*, is the residual lack of closure error.

†All data sets used for the SIR phasing were collected at room temperature. The native data set was obtained by merging a data set collected on an Raxis-II imaging plate mounted on a Rigaku (Molecular Structure, Houston) rotating anode with a data set collected on a MarResearch (MAR Research, Hamburg) imaging plate at the X31 beam line of the Deutsches Elektronen Synchrotron/European Molecular Biology Laboratory synchrotron (Hamburg). PCMB is *p*-chloromercury benzoate. The soaking time was 12 h using a saturated solution.

Table 2. Model refinement statistics

Statistics	Value
No. of nonhydrogen protein atoms*	2579 (residues 1–339)
No. of FAD and benzoate atoms	61
No. of solvent molecules	270
Resolution limits, Å	25.0–2.6 Å
R-factor, %	22.8
No. of reflections	119,237
Free *R*-factor (1000 reflections), %	24.5
rms deviation in bond lengths†,Å	0.017
rms deviation in bond angles†, degree	3.0
rms deviation in bad contacts†, Å	0.056
rms deviation B bonded atoms†, Å^2	4.6
Outliers in the Ramachandran plot‡	0

*A noncrystallographic symmetry constrain was applied in the refinement. Therefore, the eight subunits present in the asymmetric unit are identical.

†The rms deviations from the ideal values were calculated by the program TNT (18).

‡Number of residues located in the generously allowed and nonallowed regions of the Ramachandran plot according to the PROCHECK analysis (19).

binding proteins (22), the negative charge of the ribityl phosphate group is compensated by the partial positive charge associated with the N terminus of helix αF1 on the N-terminal βαβ unit (βF1–αF1–βF2, Fig. 2*b*). At the same time, the adenosine phosphate group interacts with the backbone nitrogen and the side chain hydroxyl group of two threonine residues (Thr-44 and Thr-45).

The flavin ring does not show any significant deviation from planarity and it is held in place by several interactions with the protein (Fig. 3). The N3, O4, and N5 atoms are H-bonded to the main chain of residues 49–51, located on one of the linkers connecting the FAD binding domain to the interface domain. Moreover, O2 is within H-bond distance to the backbone N atom of Thr-317, at the N terminus of helix αF5. Therefore, the fact that DAAO binds and stabilizes several anionic flavin derivatives is explained by the proximity between the N(1)—C(2)═O(2) locus and the positive charge of the helix dipole, rather than by the presence of a positively charged residue as previously postulated (28). Also, the benzene ring of the flavin extensively interacts with the protein and its two methyl groups are in van der Waals contact with Ile-202 and Gly-281. From this point of view, DAAO markedly differs from PHBH where the flavin benzene ring is exposed to the solvent (24) allowing the cofactor to adopt two different conformations within the active site (29).

The Active Site. Benzoate is a competitive inhibitor [$K_d \approx 3$ μM (5)] of DAAO being a substrate analogue. Its presence in the crystal structure allows the interpretation of the active site architecture. The inhibitor binds parallel to the flavin ring on the *re* face of the cofactor (Fig. 4*a*), as predicted by Manstein *et al.* (30). The average distance between the FAD and inhibitor planes is 3.4 Å (Fig. 4). The benzoate carboxylate group is juxtaposed to the flavin C6 atom by means of a salt bridge with the side chain of Arg-283 and a H-bond with Tyr-228 (Fig. 4*b*) in excellent agreement with the predictions based on chemical modification studies (32–34). The interactions between each one of these side chains and benzoate are very strong, as indicated by the short distances of 2.9 Å, 2.6 Å, and 2.6 Å between the inhibitor oxygen atoms and Nε-283, Nη2-283, and OH-228 atoms, respectively. In addition to these polar contacts, benzoate interacts with the side chain of Tyr-224, which stacks against the face of the benzene ring opposite to the cofactor.

Because of such extensive interactions, none of the benzoate atoms is solvent accessible. Therefore, the inhibitor binding site can be described as a cavity that is delimited by several hydrophobic side chains (Ala-49, Leu-51, Ile-215, Ile-230, Tyr-224, and Tyr-228; Fig. 4*b*) and whose access from the outside is blocked by the 216–228 loop between strands βI5 and βI6 (Fig. 2 *a* and *b*). This loop forms a lid covering the inhibitor and it is likely to be able to switch from the observed "closed" conformation to an "open" structure in order to allow substrate binding and product release. This hypothesis is supported by the following experimental observations: (*i*) product release is the rate-limiting step in the catalytic reaction (2, 5) presumably reflecting the 216–228 loop movement, and (*ii*) the peptide bond between residues 221–222 on the lid region is protected from proteolysis by the inhibitor binding (23). This suggests that in the absence of a ligand, the loop may alter its conformation, becoming susceptible to the protease action. Confirmation of this proposal must await the determination of the substrate-free enzyme structure.

The volume of the active site cavity as calculated by the program VOIDOO (31) is 160 Å^3, close to the volume occupied by an amino acid having a four carbon atoms side chain (the volume of a free Ile residue is 170 Å^3). This fact may explain why the K_m value for substrates whose side chains are formed by more than four carbon atoms is 10-fold higher than that for D-Ala (6). Modeling studies suggest in fact that a bulkier group cannot be accommodated without a significant perturbation in the substrate binding site. Furthermore, the hydrophobic nature of the side chains lining the cavity is consistent with the enzyme preference for substrates bearing hydrophobic side chains and with the very low enzymatic activity toward charged amino acids.

We have modeled an active site-bound D-Ala on the basis of the observed benzoate binding mode, assuming that the benzene ring and the carboxylate group of the inhibitor occupy the same position as the side chain and carboxylate group of the substrate, respectively (Fig. 4*b*). Furthermore, it was assumed that D-Ala is oriented such that a longer side chain would extend into the active site cavity. In the resulting model, the Cβ atom snugly fits between Cβ of Ala-49 and Cδ2 of Tyr-224, whereas the substrate α-carbon is sandwiched between atoms Cγ of Tyr-224 and N5 of the flavin, at distances of 3.5 Å and 3.4 Å, respectively. The negative charge of the substrate carboxylate group is compensated by the interactions with Arg-283 and Tyr-228 whereas the positively charged α-amino group makes a H-bond with OH of Tyr-224 and a buried solvent molecule. In the enzyme-benzoate complex, this active site water molecule further interacts with three additional ligands, the hydroxyl group of Tyr-224 and the carbonyl oxygens of Gln-53 and Gly-313, which are disposed in a nearly exact tetrahedral arrangement (Fig. 5). The water molecule has well-defined electron density in all eight subunits present in the asymmetric unit. Therefore, at this stage, it appears to be an integral part of the active site and it is likely to maintain the same location in the enzyme-substrate complex.

The model of the bound D-Ala provides insight onto enzyme stereospecificity. If the substrate amino acid were in the L-configuration and keeping the side chain location within the hydrophobic active site cavity, the α-amino group would make unfavorable contacts (<2.6 Å) with the C5a-C6 atoms of the flavin. Thus, DAAO exploits the zwitterionic nature of the amino acid to properly align it within the active site through strong polar interactions and, at the same time, achieves stereoselectivity through tight fitting of the substrate to a properly shaped binding site. In this context, it should be noticed that the substrate binding mode in DAAO is different from those observed in PHBH (24) and cholesterol oxidase (35), in spite of the similar overall topology of these proteins. In PHBH and cholesterol oxidase, the substrate lays above the cofactor and interacts with the edge of the flavin ring very differently from the face-to-face contact observed in DAAO. Therefore, these proteins appear to possess a common scaffold onto which unrelated active site architectures, suited for different types of chemical reactions, are implemented.

The Catalytic Mechanism. The catalytic properties of DAAO have been thoroughly investigated by a variety of techniques (refs. 2 and 36 and references therein). A carboanion intermediate involving abstraction of the substrate α-proton by an active site base has been proposed on the basis of the reactivity with

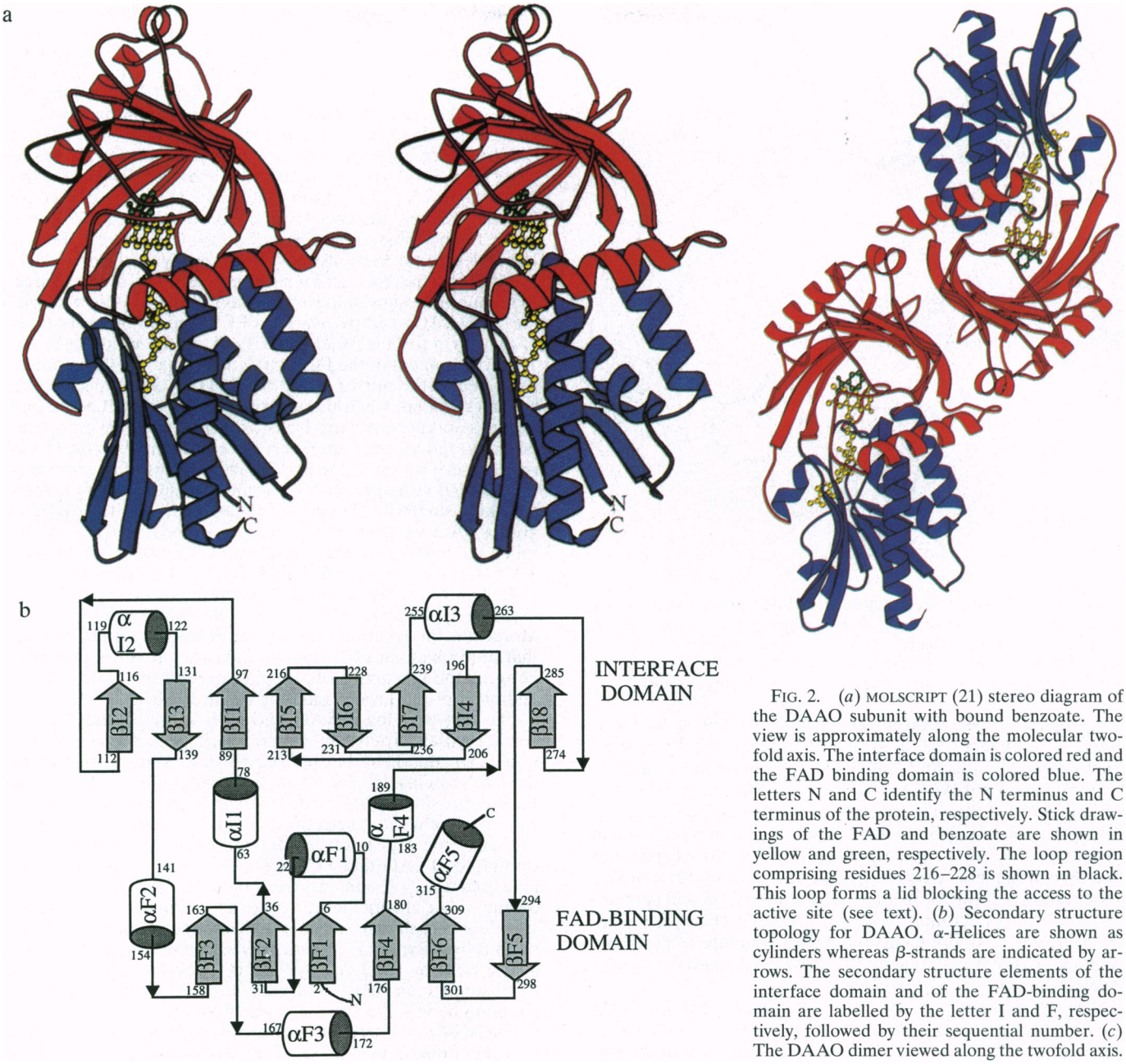

FIG. 2. (*a*) MOLSCRIPT (21) stereo diagram of the DAAO subunit with bound benzoate. The view is approximately along the molecular twofold axis. The interface domain is colored red and the FAD binding domain is colored blue. The letters N and C identify the N terminus and C terminus of the protein, respectively. Stick drawings of the FAD and benzoate are shown in yellow and green, respectively. The loop region comprising residues 216–228 is shown in black. This loop forms a lid blocking the access to the active site (see text). (*b*) Secondary structure topology for DAAO. α-Helices are shown as cylinders whereas β-strands are indicated by arrows. The secondary structure elements of the interface domain and of the FAD-binding domain are labelled by the letter I and F, respectively, followed by their sequential number. (*c*) The DAAO dimer viewed along the twofold axis.

chloro-amino acids and nitroalkanes (37). However, it has been shown that when the native FAD is replaced by 5-deaza-FAD, the α-hydrogen is directly transferred from the substrate to the C5 atom of modified cofactor (38), suggesting that flavin reduction may occur by direct transfer of the D-amino acid α-hydrogen.

The structure of DAAO in complex with benzoate reveals an active site mainly consisting of hydrophobic residues (Fig. 4*b*). The only three side-chains within 5 Å from the predicted Cα position of the substrate are Arg-283, Tyr-224, and Tyr-228. However, none of them seems properly positioned to act as the general base abstracting the substrate α-proton to generate the proposed carboanion intermediate. Arg-283 and Tyr-228 interact with the benzoate carboxylate group, whereas Tyr-224 is parallel to the benzoate ring and it forms an H-bond with the above described active site water molecule (Fig. 4*a*). In agreement with these observations, substitution of either Tyr-224 or Tyr-228 with Phe causes only a 100-fold decrease in the rate of flavin reduction (39). Moreover, primary sequence alignment comparisons show that Tyr224 is replaced by Ala in DAAO from *Rhodotorula gracilis* (40) and from *Fusarium solani* (41). Therefore, these data seem to rule out the possibility of carboanion formation initiated by one of the active site side chains acting as general base. The inhibitor-based model of the bound D-alanine shows instead that the substrate α-hydrogen points exactly toward the flavin with a Cα-N5 distance of 3.4 Å (Fig. 4*b*). This arrangement closely resembles the binding of the nicotinamide ring of pyridine nucleotides observed in several flavoenzymes (42). By analogy with these systems, a mechanism in which the flavin becomes reduced by direct transfer of the amino acid α-hydrogen to the N5 atom can be proposed (Fig. 5). The reduction can occur either via a direct hydride transfer as for the pyridine nucleotides or via a radical intermediate which does not need exact orbital overlap (42). In both cases, a proton must be released from the α-amino group of the substrate to produce the imino acid product. Such a proton can be accepted by either the Tyr-224 hydroxyl group or the active site water (Fig. 5), both groups being properly located to perform this task (Fig. 4). In this way, the reductive half-reaction is completed and the reduced FAD cofactor can donate its electrons to the final acceptor O_2, presumably by forming a C4a hydroperoxide intermediate (43). In the absence of additional structural information, no proposals for the mode of reaction between the reduced flavin and oxygen can be put forward.

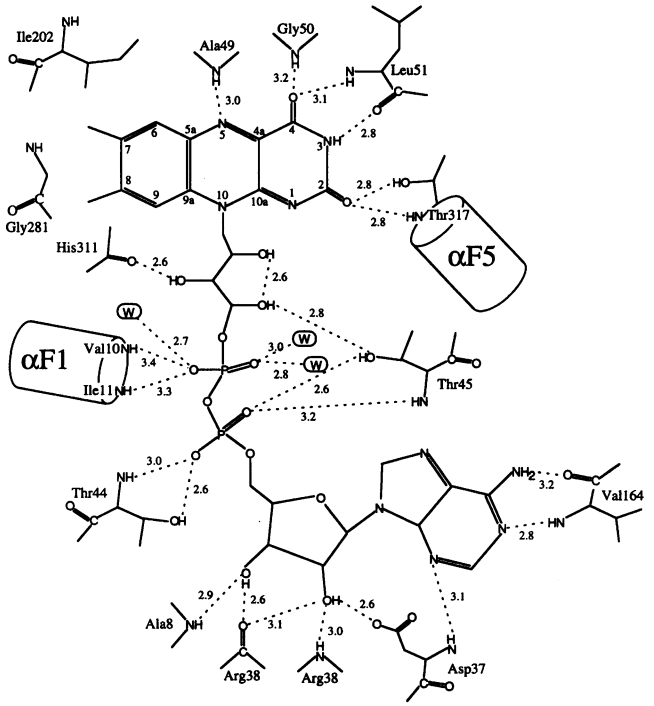

FIG. 3. Schematic representation of the FAD–DAAO interactions, outlining residues involved in hydrogen bonds to the cofactor. Water molecules present in all eight subunits in the asymmetric unit and participating in the FAD binding are indicated by W. H-bond distances are in angstroms. The numbering of the flavin atoms is shown.

Comparison with Flavocytochrome b_2. D-Amino acid oxidase is a member of a group of mechanistically related flavoenzymes displaying a number of common features, such as the reactivity toward sulfite and the ability to stabilize the anionic form of the reduced flavin derivatives (42). The group encompasses two subfamilies, the oxidases, in which flavin reoxidation occurs at the expenses of molecular oxygen, and the dehydrogenases-electron transferases that utilize a monoelectronic acceptor for oxidation. Within this second subfamily, the FMN containing flavocytochrome b_2 (FCB; L-lactate cytochrome *c* oxidoreductase) oxidizes L-lactate to pyruvate, a reaction similar to that of D-amino acid oxidase, though having opposite stereospecificity.

The crystal structure of FCB (44) shows that its flavin binding domain has a $(\beta/\alpha)_8$ topology unrelated to the structure of DAAO. However, analysis of the active site of the two proteins reveals a remarkable similarity in the nature and location of several functional groups: (*i*) the binding of the benzoate in DAAO and of pyruvate in FCB is similar; they both lay parallel to the flavin with their carboxylate groups interacting with a Tyr and an Arg side chain (Tyr-228 and Arg-283 in DAAO, Tyr-143 and Arg-376 in FCB); (*ii*) the N5 atom of the cofactor makes a H-bond with the backbone N atom of an Ala residue (Ala-49 in DAAO, Ala-198 in FCB) on the flavin side opposite to the substrate; and (*iii*) the active site water of DAAO occupies a position analogous to that of the hydroxyl group of Tyr-254 in FCB— i.e., the water of DAAO is within H-bond distance from the predicted α-amino group of the bound substrate, whereas Tyr-254 OH group in FCB is H-bonded to the carbonyl oxygen of the pyruvate product.

Although the two active sites show similar architectures, they cannot be superimposed because the locations of benzoate (in DAAO) and pyruvate (in FCB) are on opposite faces of the flavin (on the *re* side in DAAO, on the *si* side in FCB). The arrangement of the FCB catalytic groups can therefore be described as the mirror-image of the DAAO active site. This becomes evident when the coordinates of the FCB active site residues and pyruvate are transformed by applying an operation corresponding to a mirror plane coincident with the flavin ring. Superposition of the isoalloxazine atoms of the resulting mirror FCB structure onto the same atoms of DAAO reveals a striking similarity (Fig. 6) in the positioning of the catalytic groups. A rms deviation of 0.9 Å is measured when the following atom pairs are considered (DAAO/FCB): N-Ala-49/N-Ala-198, OH-Tyr-228/OH-Tyr-143, guanidinium group (Nζ, Cε, Nη1, Nη2)-Arg-283/guanidinium group-Arg-376, O-Gly-313/Nε2-His-373, active site water/OH-Tyr-254. Moreover, the location of benzoate in DAAO coincides with that of pyruvate in FCB (Fig. 6), indicating that the similarity between the two active sites applies to both substrate binding and most of the groups building the active center.

The fact that the DAAO and FCB catalytic sites can be considered as structurally enantiomeric finds a precise functional explanation in the opposite substrate stereospecificity of the two proteins. In both cases, the substrate is aligned within the binding site by a salt bridge with an arginine residue; in this way, both enzymes selectively bind the stereoisomer that properly interacts with the flavin. Thus, the topologically unrelated DAAO and FCB structures appear as a remarkable example of convergent molecular evolution toward common, but enantiomeric, active site architectures, which are suited for very similar reactions (oxidation of an α-amino acid or of an α-hydroxy acid) but with opposite stereospecificity.

The reaction catalyzed by FCB is thought to proceed via a carboanion intermediate formed after substrate proton abstraction by His-373 (refs. 42 and 45 and references therein), whereas, as discussed above, a carboanion mechanism seems now very unlikely in DAAO, which lacks a residue suited to act as the active site base abstracting the amino acid α-proton. Our

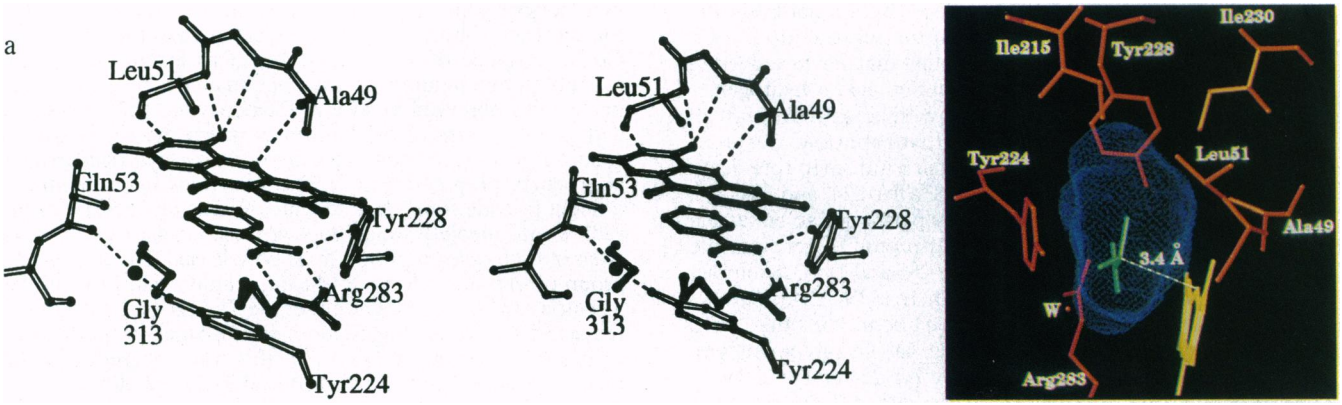

FIG. 4. (*a*) Stereo plot of the catalytic center. The "active site" water is shown as a sphere (see text). (*b*) Illustration of the active site cavity with a model for a bound D-alanine. The model was generated by optimally superposing the Cβ, Cα, and C atoms of the substrate onto the C2, C1, and carboxylate carbon of the benzoate inhibitor, respectively. The modeling was carried out using the program O (17). The blue dotted surface delineates the active site cavity and was calculated after removing the benzoate atoms from the structure (31).

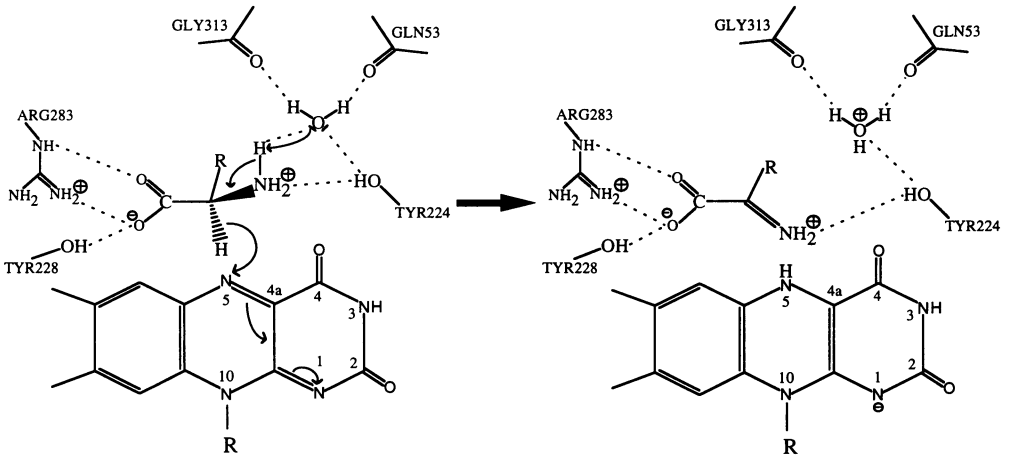

FIG. 5. Proposed mechanism for the reductive half-reaction. The α-hydrogen can be transferred to the flavin by direct hydride transfer or by a radical mechanism. In the drawing, it is shown that the proton of the substrate α-amino group is accepted by the active site water molecule. However, also the side chain of Tyr-224 could act as proton acceptor (see text).

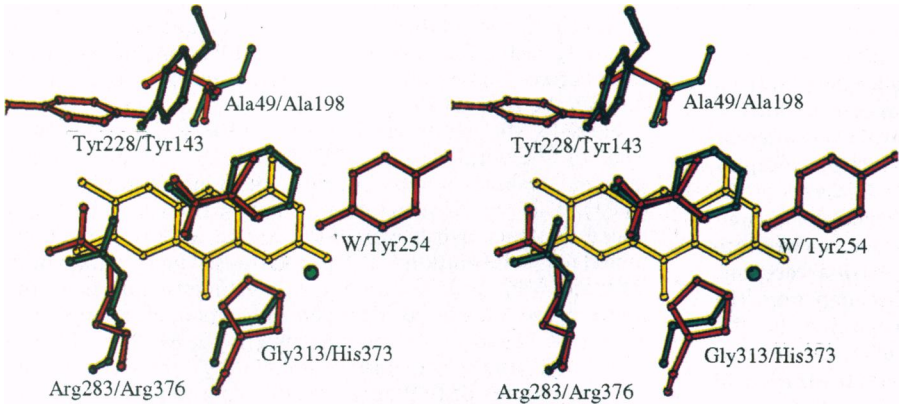

FIG. 6. Comparison between the DAAO active site (green) and the mirror-image" of the FCB catalytic center (red). FCB coordinates (44) were transformed by applying the operation corresponding to a mirror coplanar to the flavin ring. The isoalloxazine atoms of the resulting mirror FCB structure were then optimally superposed to the equivalent atoms of DAAO. The picture outlines the strikingly similar location in three-dimensional space of the catalytic groups in the two active sites. The picture was produced by using the second subunit of the FCB crystal structure (Protein Data Bank entry 1FCB).

finding that DAAO and FCB represent a case of mirror-image convergent evolution provides the basis for further experiments addressing specific questions concerning the chemical properties of these two flavoenzymes.

We thank Prof. H. L. Monaco and all members of the Pavia protein crystallography group for many useful discussions. We are grateful to Prof. P. G. Righetti and Dr. E. Wenisch for having carried out analytical and preparative isoelectrophoresis experiments and to Dr. A. Cosma, Dr. D. Mazzeo, and Prof. L. Ungaretti for their help in various phases of the project. This research was supported by grants from Ministero per l' Università e la Ricerca Scientifica e Tecnologica (MURST; 60% to B.C. and A.C.) and Consiglio Nazionale delle Ricerche (Contract 9502988CT14 to B.C. and Contract 9502989CT14 to A.M.). We thank the European Union for support of the work at the European Molecular Biology Laboratory (Hamburg) through the Human Capital Mobility Program to Large Installations Project, Contract CHGE-CT93-0040.

1. Krebs, H. A. (1935) *Biochem. J.* **29,** 1620–1625.
2. Curti, B., Ronchi, S. & Pilone Simonetta, M. (1992) in *Chemistry and Biochemistry of Flavoenzymes*, ed. Müller F. (CRC, Boca Raton, FL), pp. 69–94.
3. Ronchi, S., Minchiotti, L., Galliano, M., Curti, B., Swenson, R. P., Williams, C. H., Jr., & Massey, V. (1982) *J. Biol. Chem.* **257,** 8824–8829.
4. Momoi, K., Fukui, K., Watanabe, F. & Miyake, Y. (1988) *FEBS Lett.* **238,** 180–185.
5. Bright, H. J. & Porter, D. J. T. (1975) *Enzymes* **12,** 421–441.
6. Dixon, M. & Kleppe, K. (1965) *Biochim. Biophys. Acta* **96,** 368–382.
7. Negri, A., Massey, V. & Williams, C. H., Jr. (1987) *J. Biol. Chem.* **262,** 10026–10034.
8. D'Aniello, A., D'Onofrio, G., Pischetola, M., D'Aniello, G., Vetere, A., Petrucelli, L. & Fisher, G. H. (1993) *J. Biol. Chem.* **268,** 26941–26949.
9. Mor, A., Amiche, M. & Nicolas, P. (1992) *Trends Biochem. Sci.* **17,** 481–485.
10. Man, E. H., Sandhouse, M., Burg, J. & Fisher, G. H. (1983) *Science* **220,** 1407–1408.
11. Curti, B., Ronchi, S., Branzoli, U., Ferri, G. & Williams, C. H., Jr. (1973) *Biochim. Biophys. Acta* **327,** 231–266.
12. Bolognesi, M., Ungaretti, L., Curti, B. & Ronchi, S. (1978) *J. Biol. Chem.* **253,** 7513–7514.
13. Collaborative Computational Project Number 4 (1994) *Acta Crystallogr. D* **50,** 760–767.
14. Sheldrick, G. M. (1991) in *Isomorphous Replacement and Anomalous Scattering: Proceedings of the CCP4 Study Weekend 25–26 January 1991,* eds. Wolf, W., Evans, P. R. & Leslie, A. G. W. (Science and Engineering Research Lab., Daresbury Lab., Warrington, U.K.), pp. 23–38.
15. Tong, L. & Rossmann, M. G. (1990) *Acta Crystallogr. A* **46,** 783–792.
16. Vellieux, F. M. D. V., Hunt, J. F., Roy, S. & Read, R. J. (1995) *J. Appl. Crystallogr.* **28,** 347–351.
17. Jones, T. A., Zou, J. Y., Cowan, S. W. & Kjeldgaard, M. (1991) *Acta Crystallogr. A* **47,** 110–119.
18. Tronrud, D. E., Ten Eyck, L. F. & Matthews, B. W. (1987) *Acta Crystallogr. A* **43,** 489–501.
19. Laskowski, R. A., MacArthur, M. W., Moss, D. S. & Thornton, J. M. (1993) *J. Appl. Crystallogr.* **26,** 283–291.
20. Brünger, A. T. (1992) *Nature (London)* **355,** 472–475.
21. Kraulis, P. J. (1991) *J. Appl. Crystallogr.* **24,** 946–950.
22. Wierenga, R. K., Drenth, J. & Schulz, G. E. (1983) *J. Mol. Biol.* **167,** 725–739.
23. Torri Tarelli, G., Vanoni, M. A., Negri, A. & Curti, B. (1990) *J. Biol. Chem.* **34,** 21242–21246.
24. Schreuder, H. A., Prick, P. A. J., Wierenga, P. K., Vriend, G., Wilson, K. S., Hol, W. G. J. & Drenth, J. (1989) *J. Mol. Biol.* **208,** 679–696.
25. Vrielink, A., Lloyd, L. F. & Blow, D. M. (1991) *J. Mol. Biol.* **219,** 533–554.
26. Hecht, H. J., Kalisz, H. M., Hendle, J., Schmid, R. D. & Schomburg, D. (1993) *J. Mol. Biol.* **229,** 153–172.
27. Holm, L. & Sander, C. (1993) *J. Mol. Biol.* **233,** 123–138.
28. Ghisla, S. & Massey, V. (1986) *Biochem. J.* **239,** 1–12.
29. Entsch, B. & van Berkel, W. J. H. (1995) *FASEB J.* **9,** 476–483.
30. Manstein, D. J., Massey, V., Ghisla, S. & Pai, E. F. (1988) *Biochemistry* **27,** 2300–2303.
31. Kleywegt, G. J. & Jones, T. A. (1994) *Acta Crystallogr. D* **50,** 178–185.
32. Ronchi, S., Galliano, M., Minchiotti, L., Curti, B., Rudie, N. G., Porter, D. J. T. & Bright, H. J. (1980) *J. Biol. Chem.* **255,** 6044–6050.
33. Ferti, C., Curti, B., Pilone Simonetta, M., Ronchi, S., Galliano, M. & Minchiotti, L. (1981) *Eur. J. Biochem.* **119,** 553–557.
34. Gadda, G., Negri, A. & Pilone, M. S. (1994) *J. Biol. Chem.* **269,** 17809–17814.
35. Li, J., Vrielink, A., Brick, P. & Blow, D. (1993) *Biochemistry* **32,** 11507–11515.
36. Denu, J. M. & Fitzpatrick, P. F. (1994) *Biochemistry* **33,** 4001–4007.
37. Walsh, C. T., Krodel, E., Massey, V. & Abels, R. H. (1973) *J. Biol. Chem.* **248,** 1946–1951.
38. Hersh, L. B. & Schuman Jorns, M. (1975) *J. Biol. Chem.* **250,** 8728–8732.
39. Pollegioni, L., Fukui, K. & Massey, V. (1994) *J. Biol. Chem.* **269,** 31666–31673.
40. Faotto, L., Pollegioni, L., Ceciliani, F., Ronchi, S. & Pilone, M. S. (1995) *Biotechnol. Lett.* **17,** 193–198.
41. Isolai, T., Ono, H., Ishitani, Y., Kojo, H., Veday, Y., Kohsaka, M. (1994) *J. Biochem. (Tokyo)* **108,** 1063–1069.
42. Ghisla, S. & Massey, V. (1989) *Eur. J. Biochem.* **181,** 1–17.
43. Massey, V. (1994) *J. Biol. Chem.* **269,** 22459–22462.
44. Xia, Z. X. & Mathews, F. S. (1990) *J. Mol. Biol.* **212,** 837–863.
45. Lederer, F. (1992) *Protein Sci.* **1,** 540–548